Identification of the C═O Stretching Vibrations of FMN and Peptide Backbone by ^{13}C-Labeling of the LOV2 Domain of *Adiantum* Phytochrome3

Tatsuya Iwata,[‡] Dai Nozaki,[‡] Yoshiaki Sato,[‡] Kyosuke Sato,[§] Yasuzo Nishina,[||] Kiyoshi Shiga,[§] Satoru Tokutomi,[⊥] and Hideki Kandori*[,‡]

Department of Materials Science and Engineering, Nagoya Institute of Technology, Showa-ku, Nagoya 466-8555, Japan, Department of Molecular Physiology, Graduate School of Medical Sciences, Kumamoto University, Honjo, Kumamoto 860-8556, Japan, Department of Physiology, School of Health Sciences, Kumamoto University, Kuhonji, Kumamoto 862-0976, Japan, and Department of Biological Science, Graduate School of Science, Osaka Prefecture University, Sakai, Osaka 599-8531, Japan

Received September 1, 2006; Revised Manuscript Received October 29, 2006

ABSTRACT: Phototropin, a blue-light photoreceptor in plants, has two FMN-binding domains named LOV1 and LOV2. We previously observed temperature-dependent FTIR spectral changes in the C═O stretching region (amide-I vibrational region of the peptide backbone) for the LOV2 domain of *Adiantum* phytochrome3 (phy3-LOV2), suggesting progressive structural changes in the protein moiety (Iwata, T., Nozaki, D., Tokutomi, S., Kagawa, T., Wada, M., and Kandori, H. (2003) *Biochemistry 42*, 8183−8191). Because FMN also possesses two C═O groups, in this article, we aimed at assigning C═O stretching vibrations of the FMN and protein by using ^{13}C-labeling. We assigned the C(4)═O and C(2)═O stretching vibrations of FMN by using [4,10a-$^{13}C_2$] and [2-^{13}C] FMNs, respectively, whereas C═O stretching vibrations of amide-I were assigned by using ^{13}C-labeling of protein. We found that both C(4)═O and C(2)═O stretching vibrations shift to higher frequencies upon the formation of S390 at 77−295 K, suggesting that the hydrogen bonds of the C═O groups are weakened by adduct formation. Adduct formation presumably relocates the FMN chromophore apart from its hydrogen-bonding donors. Temperature-dependent amide-I bands are unequivocally assigned by separating the chromophore bands. The hydrogen bond of the peptide backbone in the loop region is weakened upon S390 formation at low temperatures, while being strengthened at room temperature. The hydrogen bond of the peptide backbone in the α-helix is weakened regardless of temperature. On the other hand, structural perturbation of the *β*-sheet is observed only at room temperature, where the hydrogen bond is strengthened. Light-signal transduction by phy3-LOV2 must be achieved by the progressive protein structural changes initiated by the adduct formation of the FMN.

Phototropin is a blue-light receptor in plants, which is involved in physiological responses, such as the phototropic response (*1*), relocation of chloroplasts (*2*), and stomata opening (*3*). Phototropin possesses two flavin mononucleotide (FMN[1]) binding domains on the *N*-terminal side and a Ser/Thr kinase motif on the *C*-terminal side. Blue-light absorption by the chromophore domain thereby leads to the regulation of kinase activity, probably through the change in domain−domain interaction. The FMN-binding chromophoric domain in primary (*4*) and tertiary (*5*) structures is highly homologous to bacterial light-sensor PYP (photoactive yellow protein), oxygen-sensor FixL, and voltage-sensor HERG of a channel protein so that the domain is called the LOV (light, oxygen, and voltage sensing) domain. The protein fold belongs to the PAS (Per-Arnt-Sim) superfamily. Previous X-ray crystallography showed that the structures of two LOV domains, LOV1 and LOV2, in the phototropin are very similar from the analysis of the LOV2 domain of *Adiantum* phytochrome 3 (phy3) (Figure 1a) (*5*) and the LOV1 domain of *Chlamydomonas* phot (*6*).

The photoreaction in the LOV domain is an adduct formation between the FMN and a nearby cysteine (Figure 1b) (*7*−*11*). Following light absorption by the FMN, intersystem crossing leads to the formation of a triplet excited state absorbing at 660 nm (L660), appearing with a time constant of 3 ns in *Adiantum* phy3-LOV2 and oat phot1-LOV2 (*12*). Then, adduct formation accompanies the appearance of the S390 intermediate with a time constant of 4 *μ*s in oat phot1-LOV2 (*9*) and with 0.9 and 4 *μ*s in *Chlamydomonas* phot-LOV1 (*13*). Although various models have been proposed for the reactive cysteine, previous FTIR studies revealed that the cysteine is protonated both in the ground (*14*−*17*) and triplet excited (*18*) states of the FMN. Dynamical protein motion probably plays an important role in adduct formation (*19*).

S390 is the only ground-state intermediate during the photocycle of LOV domains. Therefore, it is believed that

* To whom correspondence should be addressed. Phone: 81-52-735-5207. Fax: 81-52-735-5207. E-mail: kandori@nitech.ac.jp.
[‡] Nagoya Institute of Technology.
[§] Graduate School of Medical Sciences, Kumamoto University.
[||] School of Health Sciences, Kumamoto University.
[⊥] Osaka Prefecture University.

[1] Abbreviations: FMN, flavin mononucleotide; LOV, light-oxygen-voltage; PAS, Per-Arnt-Sim; FTIR, Fourier transform infrared.

10.1021/bi061837v CCC: $33.50
Published on Web 12/05/2006

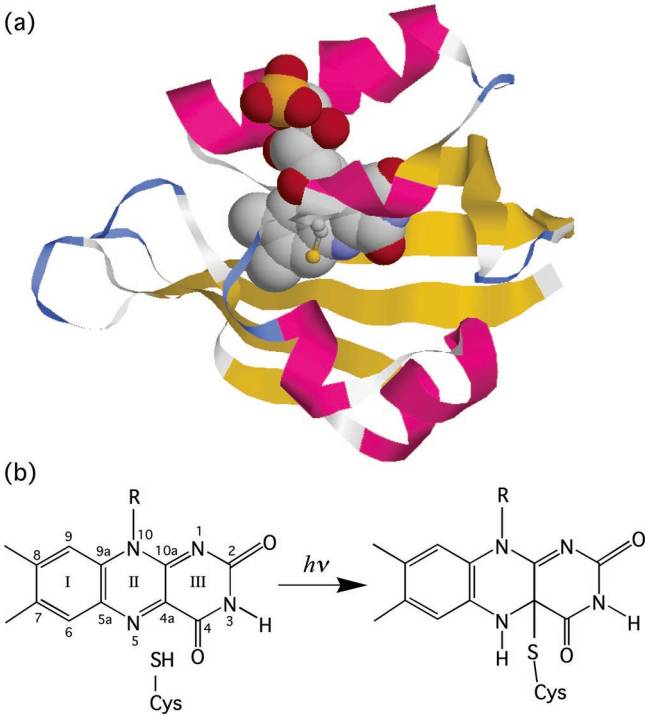

FIGURE 1: (a) Protein structure of phy3-LOV2 (pdb entry 1G28) (*7*). The whole structure is shown as a ribbon drawing, where helices, turns, and sheets are colored red, blue, and yellow, respectively. The FMN is shown as a space-filling drawing, whereas Cys966 is shown as a ball-and-stick drawing. The folding motif of this protein is characteristic of the PAS superfamily. (b) Photoreaction scheme for the LOV domains.

S390 is the active state for the light-sensing function of phototropin. Although the surface structures are identical between the crystal structures of the unphotolyzed (*5*) and S390 (*11*) states of phy3-LOV2, our FTIR study showed the highly temperature-dependent nature of the amide-I vibrations of phy3-LOV2. At 150 K, prominent positive peaks appeared at 1692 and 1687 cm^{-1} (see Figure 7 of ref 20 (*20*), which is reproduced in the Figures in this article). The peak at 1692 cm^{-1} disappears completely at 295 K, whereas a new peak appears at 1629 cm^{-1}. The former and latter vibrations are ascribable to the amide-I vibrations of the loop region and β-sheet, respectively. On the basis of these observations, we attributed the progressive protein structural changes taking place from the loop region near Cys966 to the β-sheet. We also suggested that the structural changes of the β-sheet probably accompany the change in the protein surface, though not observed by X-ray crystallography. Interestingly, such structural changes of the β-sheet were not observed for the Q1029L mutant, implying that Gln1029 has an important role in the intramolecular signaling of phy3-LOV2 (*21*). Gln1029, involved in a β-sheet region, is located between an FMN and an extra helix (called Jα) that is largely changed in the light-activated state (*22*, *23*). Thus, the light signal is presumably relayed from FMN to Jα through the β-sheet (Gln1029) in LOV domains.

It should be noted that the frequency region of amide-I vibrations (1700−1600 cm^{-1}) also contains the C═O stretching vibrations of FMNs. According to the literature, the C(4)═O and C(2)═O stretching vibrations of FMNs are located at ∼1700 and ∼1680 cm^{-1}, respectively (*24*−*28*), which might be different in protein. This indicates that a better understanding of protein structural changes demands the complete assignment of the C═O stretching vibrations of the FMN and protein. In fact, different arguments have been provided in previous FTIR studies. Ataka et al. concluded that the signal in this region originates from the FMN and that amide-I vibrations are absent in the difference spectra of *Chlamydomonas* phot-LOV1 (*15*). In contrast, Swartz et al. concluded the certain contribution of amide-I vibrations in the difference spectra of oat phot1-LOV2 (*29*). These could not be inconsistent with each other because our recent comparative study of phy3-LOV1 and phy3-LOV2 revealed that protein structural changes are smaller for LOV1 than for LOV2 (*17*). In any case, a clear view is obtained only when signals from the FMN and protein are separated.

In this article, we attempted to separate the C═O stretching vibrations of the FMN and protein by using ^{13}C-labeling. To this end, we first established the reconstitution method of the FMN chromophore with high yield. Then, to assign the C═O stretching vibrations of FMN, we synthesized isotope-labeled chromophores, such as [4,10a-$^{13}C_2$] and [2-^{13}C] FMNs. The FTIR measurements of these labeled FMNs led to the unequivocal assignment of the C(4)═O and C(2)═O stretching vibrations. ^{13}C-labeling of the protein allowed us to separate the C═O stretching vibrations of the peptide backbone (amide-I bands) from those of the FMN.

MATERIALS AND METHODS

Preparation of Adiantum phy3-LOV2. The phy3-LOV2 construct in the present experiment contains *N*-terminal calmodulin-binding peptide and spanning amino acid residues Pro905−Pro1087 of phy3, which include Jα helix (Asp1050−Arg1072) (*20*, *21*). The phy3-LOV2 domain was prepared as described previously (*20*, *21*) except for the growth medium used. *Escherichia coli* BL21(DE3) was grown in an M9 minimum medium. For universal ^{13}C-labeling, ^{13}C-glucose (Shoko Tsusho) was used at a concentration of 4 g/L.

Reconstitution of the FMN and Protein. Purified phy3-LOV2 was rebound to a column of Calmodulin resin, which was equilibrated with a $CaCl_2$ binding buffer (50 mM Tris-HCl (pH 8.0), 2 mM $CaCl_2$, 1 mM $Mg(CH_3COO)_2$, 10 mM 2-mercaptoethanol (2-ME), and 50 mM NaCl). The FMN in the protein was removed by buffer A (50 mM KH_2PO_4 (pH 4.0), 2 mM $CaCl_2$, 1 mM $Mg(CH_3COO)_2$, 10 mM 2-ME, and 150 mM NaCl) until the absorbance at 280 nm became zero. Then, the column was washed by the $CaCl_2$ binding buffer. A solution containing twice the molar excess of the FMN in the $CaCl_2$ binding buffer was recycled through the column for 18 h at a flow rate of 1 mL/min at 4 °C. The column was washed with the $CaCl_2$ binding buffer, and the protein was eluted by a NaCl elution buffer (50 mM Tris-HCl (pH 8.0), 2 mM EGTA, 10 mM 2-ME, and 1 M NaCl). The yield of the chromophore reconstitution was estimated to be 60−70%. Two kinds of site-directed ^{13}C-labeled FMNs, [4,10a-$^{13}C_2$]FMN and [2-^{13}C]FMN, were synthesized as described previously (*30*, *31*). The yields of labeling were >90%.

FTIR Measurements. FTIR measurements were carried out as described elsewhere (*20*, *21*). Infrared spectra of the hydrated films were measured using an FTS-7000 (Bio-Rad) spectrophotometer. Hydrated films were illuminated by a >400 nm light, which was supplied by a combination of a

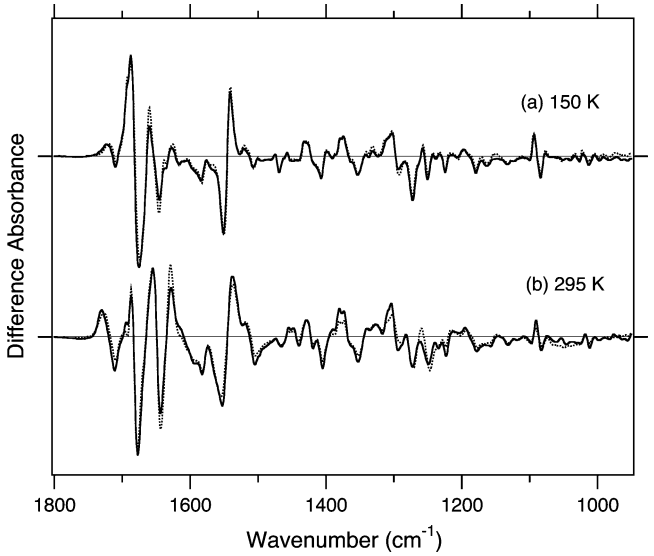

FIGURE 2: Difference FTIR spectra of native phy3-LOV2 (dotted lines) and phy3-LOV2 reconstituted with the FMN and apoprotein (solid lines) in the 1800−950 cm^{-1} region at 150 K (a) and 295 K (b). One division of the *y*-axis corresponds to 0.008 absorbance units.

halogen−tungsten lamp (1000 W) and a long-pass filter (L42, Asahi Techno Glass). In this way we obtained light-induced difference spectra, either at 150 or 295 K.

RESULTS

Reconstitution of the FMN Chromophore into the phy3-LOV2 Apoprotein. We first examined whether the FMN chromophore is properly reconstituted into the original binding site. Figure 2 compares difference IR spectra of the S390 and unphotolyzed states between the native (dotted lines) and reconstituted (solid lines) phy3-LOV2 measured at 150 K (a) and 295 K (b). The reconstituted phy3-LOV2 sample was prepared by mixing the unlabeled FMN and apoprotein as described in Materials and Methods. Both spectra at 150 K (Figure 2a) coincide very well with each other, indicating that the FMN chromophore is properly reconstituted into the binding pocket. In fact, identical absorption spectra in the UV−visible region and similar photoreaction kinetics were obtained for the native and reconstituted phy3-LOV2 (data not shown). The difference IR spectra are also similar at 295 K (Figure 2b), although the spectral deviation was larger at 295 K than at 150 K. This fact may indicate that reconstitution of the FMN does not necessarily yield natively folding phy3-LOV2. Figure 2 provides criteria of experimental accuracy in the following measurements.

^{13}C Isotope Effect of the FMN for the Vibrations at 1600−950 cm^{-1}. Figure 3a shows difference IR spectra of phy3-LOV2 reconstituted with unlabeled FMN (solid line) and [4,10a-$^{13}C_2$]FMN (dotted line) measured at 150 K. In the 1600−950 cm^{-1} region, the following bands exhibit an isotope effect; 1584 (−), 1551 (−), 1541 (+), 1521 (+), 1507 (−), 1432 (+), 1407 (−), 1379 (+), 1353 (−), 1258 (+), and 1250 (−) cm^{-1}. A similar isotope effect was observed at 295 K with slightly modified frequencies (Figure 3b). This fact implies that the structural change of the FMN is identical at 150 and 295 K, which confirms the statement in our previous article (*20*).

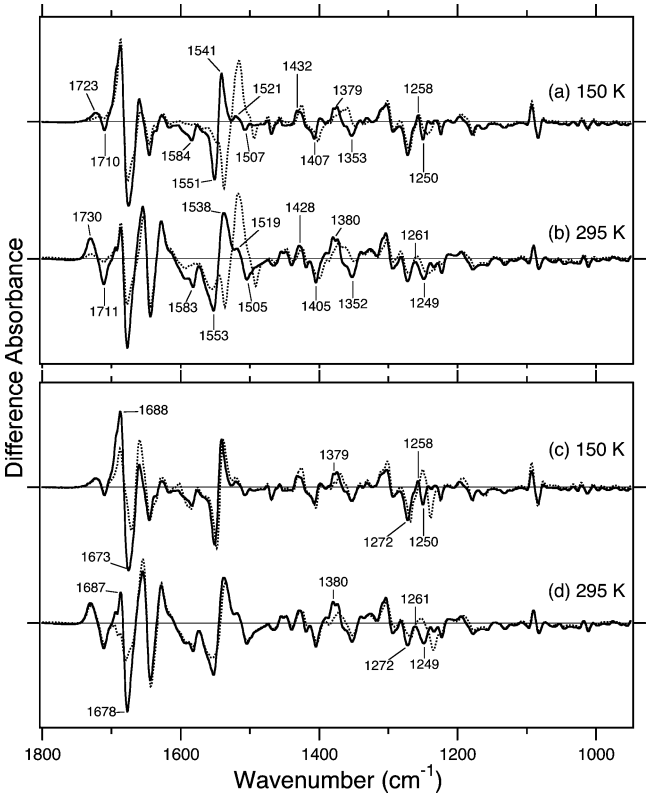

FIGURE 3: (a and b) Difference FTIR spectra of phy3-LOV2 reconstituted with unlabeled FMN (solid lines) and [4, 10a-$^{13}C_2$]-FMN (dotted lines) in the 1800−950 cm^{-1} region at 150 K (a) and 295 K (b). (c and d) Difference FTIR spectra of phy3-LOV2 reconstituted with unlabeled FMN (solid lines) and [2-^{13}C]FMN (dotted lines) in the 1800−950 cm^{-1} region at 150 K (c) and 295 K (d). Spectra are normalized by a negative band at ∼2568 cm^{-1} (S−H stretching vibration of Cys966). One division of the *y*-axis corresponds to 0.008 absorbance units.

The negative 1584 cm^{-1} band disappears for [4,10a-$^{13}C_2$]-FMN. Previous normal-mode analysis of FMN (*28*) and lumiflavin (*24*−*27*) assigned this band to the coupled mode of the C(10a)═N(1) and C(4a)═N(5) stretching vibrations. Using resonance Raman spectroscopy of labeled riboflavin, Kitagawa et al. showed that the 1584 cm^{-1} band originates mainly from C(4a)═N(5) stretching (*32*) (Table 1). The introduction of the ^{13}C atom at position C(10a) should decouple the vibrational mode, explaining the observed lack of the 1584 cm^{-1} band. On the other hand, the negative bands at 1551 and 1507 cm^{-1} exhibit isotope shifts by 14 cm^{-1}.

Table 1: Assignment of Vibrational Bands for phy3-LOV2

150 K		295 K		
unphotolyzed	S390	unphotolyzed	S390	assignment
1710	1723	1711	1730	C(4)═O stretch of FMN
1673	1692	1678	1655	amide-I (loop)
1677	1687	1677	1686	C(2)═O stretch of FMN
1646	1660	1644	1655	amide-I (α-helix)
		1644	1629	amide-I (*β*-sheet)
1584		1583		C(4a)═N(5) stretch of FMN
1551	1541	1553	1538	C(10a)═N(1) stretch of FMN
		1553	1538	amide-II
1507	1521	1505	1519	C(10a)═N(1) stretch of FMN

Previous normal-mode analysis reported that these vibrations contain atomic displacement of C(10a) (*24*−*28*). Therefore, these vibrations are presumably attributable to coupled vibrations containing the C(10a)═N(1) stretching mode (Table 1). The negative bands at 1407, 1353, and 1250 cm^{-1} exhibit isotope shifts by 5−7 cm^{-1} for [4,10a-$^{13}C_2$]FMN (Figure 3a and b). Lower frequencies suggest that these vibrations contain single band characters of FMN, such as C(4)−N(3), C(4)−C(4a), C(4a)−C(10a), and C(10a)−N(10) stretches. Such an assignment is consistent with those from previous studies (*15*, *24*−*28*).

The positive band at 1541 cm^{-1} exhibits an isotope shift by 25 cm^{-1}, which probably corresponds to the negative band at 1551 cm^{-1}. It is also likely that the ^{13}C-labeling at position 4 and 10a affects the band at 1521 cm^{-1}. Previous normal-mode analysis reported the presence of two vibrations in this frequency region: the antisymmetric (higher frequency) and symmetric (lower frequency) C(10a)═N(1) stretches coupled with the C(5a)═C(9a) stretch (*29*). Therefore, both bands at 1541 and 1521 cm^{-1} contain the C(10a)═N(1) stretching vibration in the adduct. Positive bands at 1432, 1379, and 1258 cm^{-1} downshifted by 4−12 cm^{-1} by isotope substitution, which probably correspond to the negative bands at 1407, 1353, and 1250 cm^{-1}, respectively. Previous normal-mode analysis reported that these bands originate from ring stretching vibrations (*29*).

Figure 3c shows the difference IR spectra of phy3-LOV2 reconstituted with unlabeled FMN (solid line) and [2-^{13}C]-FMN (dotted line) measured at 150 K. The observed isotope effect was less than that for [4,10a-$^{13}C_2$]FMN, possibly because of the labeling of a single atom. At <1600 cm^{-1}, we observed the shifted bands at 1379 (+), 1272 (−), 1258 (+), and 1250 (−) cm^{-1}. As in the case of [4,10a-$^{13}C_2$]FMN, a similar isotope effect was observed at 295 K with slightly modified frequencies (Figure 3d), implying that the structural change of the FMN is identical at 150 and 295 K.

The negative bands at 1272 and 1250 cm^{-1} in Figure 3c exhibit isotope shifts by 4 and 11 cm^{-1}, respectively, between which the latter also shows a spectral downshift for [4,10a-$^{13}C_2$]FMN (Figure 3a). These bands contain the vibrational mode of C(2)−N(1) or C(2)−N(3) of the FMN in the unphotolyzed state. The positive bands at 1379 and 1258 cm^{-1} exhibit isotope shifts by 10 and 7 cm^{-1}, respectively. These bands can be assigned to ring stretching vibrations that contain displacement of the C(2) atom.

^{13}C Isotope Effect of FMN for the Vibrations at 1800−*1600 cm^{-1}.* C═O stretching vibrations of the FMN and peptide backbone (amide-I) appear at 1800−1600 cm^{-1}. The bands at 1730−1710 cm^{-1} are attributable to the C(4)═O stretching vibration because a clear isotope effect was observed for [4,10a-$^{13}C_2$]FMN (Figure 3a and b) but not for [2-^{13}C]FMN (Figure 3c and d). The bands at 1723 (+)/1710 (−) cm^{-1} (Figure 3a) and 1730 (+)/1711 (−) cm^{-1} (Figure 3b) were not observed by ^{13}C labeling of the C(4)═O group, probably because they downshifted. The remaining bands (∼15%) may originate from incomplete reconstitution of FMN. For substitution of ^{12}C to ^{13}C, the spectral downshift is expected to be 35−40 cm^{-1}, calculated from the square root of reduced mass ratio between ^{12}C═O and ^{13}C═O (dotted lines in Figure 3a and b). Because strong bands of amide-I vibrations mask such shifted bands, we examined the detailed isotope shift by calculating double difference

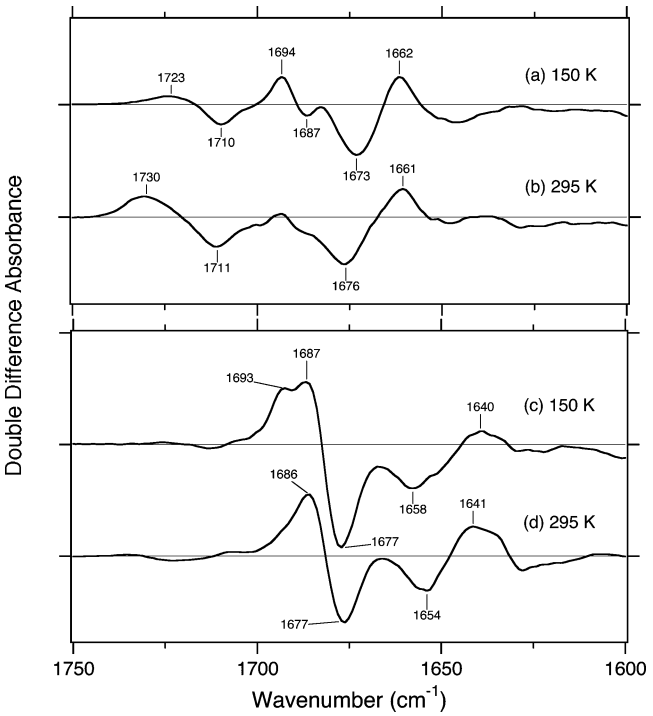

FIGURE 4: Double-difference spectra of those in Figure 4, where the labeled spectra (dotted lines) are subtracted from the unlabeled spectra (solid lines). The labeled chromophores are [4, 10a-$^{13}C_2$]-FMN (a and b) and [2-^{13}C]FMN (c and d). One division of the *y*-axis corresponds to 0.004 absorbance units.

spectra. Figure 4a shows the double difference spectrum at 150 K, where the labeled spectrum (dotted line in Figure 3a) was subtracted from the unlabeled one (solid line in Figure 3a). Such spectral analysis indicates that the bands at 1723 (+) and 1710 (−) cm^{-1} exhibit downshifts to 1673 and 1662 cm^{-1} by ^{13}C(4) labeling, respectively (Table 1). A larger spectral downshift (about 50 cm^{-1}) was also observed for FMN in solution and explained in terms of vibrational coupling of the C(4)═O stretch and the N(3)−H bend for the FMN in solution (*31*). The origin of the bands at 1694 (+)/1687 (−) cm^{-1} in Figure 4a is unclear. Large absorption in this frequency region might perturb the spectra. The double difference spectrum at 295 K also shows a similar spectral feature of the isotope effect, although lacking additional bands at about 1690 cm^{-1} (Figure 4b).

Figure 3c and d show significant isotope effects at 1700−1650 cm^{-1} for the ^{13}C-labeling at the C(2) position. Corresponding double difference spectra are shown in Figure 4c and d. As clearly shown in Figure 4d, the C(2)═O stretching vibrations of the unphotolyzed and S390 states can be assigned to the 1677 and 1686 cm^{-1} bands, which shift to 1641 and 1654 cm^{-1}, respectively. Isotope shifts are smaller than those for the C(4)═O stretch, which may suggest that the C(2)═O stretch is an isolated mode. The presence of the positive band at 1693 cm^{-1} at 150 K is unclear at present. It does not probably originate from the C(2)═O stretch because the ^{13}C-labeling of protein entirely shifts the band at 1693 cm^{-1}. In fact, ^{13}C-labeling of protein separates the C═O stretching vibrations of FMN and protein, which will be shown below.

^{13}C Isotope Effect of Protein for the Vibrations at 1600−*950 cm^{-1}.* We then introduced ^{13}C-labeling into the protein of phy3-LOV2. Figure 5a shows the difference FTIR spectra

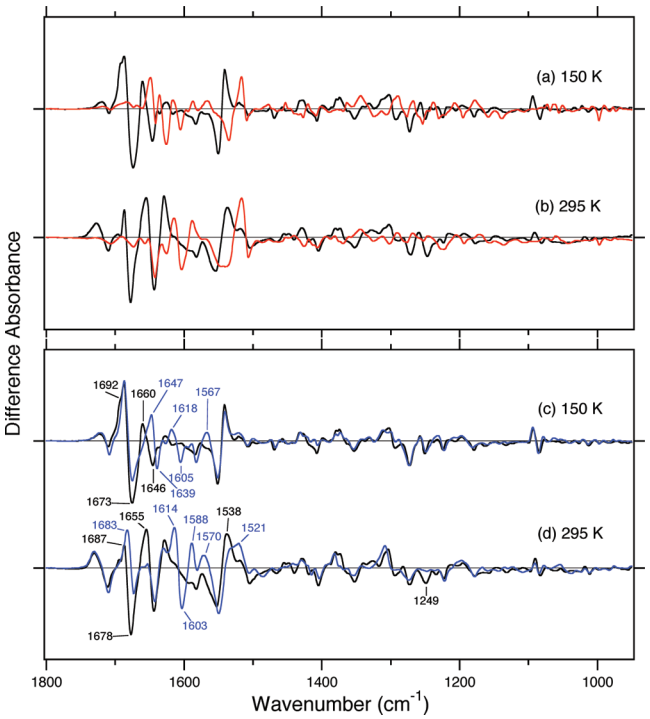

FIGURE 5: (a and b) Difference FTIR spectra of native phy3-LOV2 (black lines) and uniformly ^{13}C-labeled (^{13}C-FMN/^{13}C-apoprotein) phy3-LOV2 (red lines) in the 1800−950 cm^{-1} region at 150 K (a) and 295 K (b). (c and d) Difference FTIR spectra of phy3-LOV2 reconstituted with unlabeled FMN to unlabeled (black lines) and ^{13}C-labeled (blue lines) apoprotein in the 1800−950 cm^{-1} region at 150 K (c) and 295 K (d). Spectra are normalized by a negative band at ∼2568 cm^{-1} (S−H stretching vibration of Cys966). One division of the *y*-axis corresponds to 0.008 absorbance units.

of uniformly ^{13}C-labeled (red lines) and unlabeled (black lines) phy3-LOV2 at 150 K, whereas Figure 5b shows those at 295 K. Figure 5a and b show that the signal of ^{13}C-labeled phy3-LOV2 is completely different from that of unlabeled phy3-LOV2, indicating that most of the vibrational bands contain atomic displacement of carbon.

Figure 5c shows the difference FTIR spectra of phy3-LOV2 reconstituted with unlabeled FMN at 150 K, where apoprotein is ^{13}C-labeled (blue lines) and unlabeled (black lines). Unlike in Figure 5a, the blue and black lines coincide well with each other, particularly at 1600−950 cm^{-1}. This fact indicates that most of the vibrational bands in this frequency region originate from FMN, not from protein. The peak at 1567 cm^{-1} probably originates from amide-II vibrations. Although a similar tendency was seen at 295 K (Figure 5d), spectral deviation at 1600−950 cm^{-1} was clearly larger at 295 K than at 150 K. This indicates that protein structural changes are larger at room temperature, confirming the conclusions of our earlier work (*20*). Spectral differences at 1570−1520 cm^{-1} (Figure 5c and d) and 1300−1200 cm^{-1} (Figure 5d) are attributable to the amide-II and amide-III vibrational modes, respectively. Interestingly, the negative band at 1249 cm^{-1} at 295 K (Figure 5d) almost completely disappears by ^{13}C-labeling of the protein. This is also shifted or missing for [4,10a-$^{13}C_2$] (Figure 3b) or [2-^{13}C] (Figure 3d) labeling of FMN, respectively. This frequency region contains both chromophore and protein vibrations, and we have to be careful in assigning vibrational bands.

^{13}C Isotope Effect of Protein for the Vibrations at 1800−1600 cm^{-1}. The most prominent isotope effect in Figure 5c and d was seen for the amide-I region at 1800−1600 cm^{-1}. Figure 5c shows that the bands of the unlabeled protein at 1692 (+), 1660 (+), and 1646 (−) cm^{-1} disappeared (black lines), whereas the bands at 1647(+), 1639 (−), 1618 (+), and 1605 (−) cm^{-1} newly appeared for the ^{13}C-labeling of protein (blue lines) at 150 K. The signal intensity at 1673 (−) cm^{-1} in Figure 5c was reduced upon ^{13}C-labeling of the protein. The spectral feature is remarkably different at 295 K, where ^{13}C═O bands appeared at 1614 (+), 1603 (−), 1588 (+), and 1570 (+) cm^{-1} (blue line in Figure 5d) more strongly than those at 150 K. We analyze the spectra in more detail below.

Figure 6 shows a close up look at the difference IR spectra at 150 K (a) and 295 K (b), where the corresponding bands for the ^{12}C and ^{13}C samples were connected by dotted lines. In Figure 6a, the bands at 1723 (+), 1710 (−), and 1688 (+) cm^{-1} were not shifted for ^{13}C-labeling of the protein. On the other hand, the bands at 1692 (+), 1673 (−), 1660 (+), and 1646 (−) cm^{-1} exhibited an isotope effect, presumably shifting to 1647 (+), 1639 (−), 1618 (+), and 1605 (−) cm^{-1}, respectively. The band at 1673 (−) cm^{-1} was split into two bands for ^{13}C-labeling of protein, the remaining band at 1675 cm^{-1} and the shifted band at 1639 (−) cm^{-1}. Thus, the blue spectrum in Figure 6a clearly demonstrates the successful separation of the bands at 1750−1650 cm^{-1} into those of the FMN and protein. As we showed in Figures 3 and 4, the bands at 1723 (+)/1710 (−) and 1687 (+)/1675 (−) cm^{-1} originate from the C(4)═O and C(2)═O stretching vibrations of FMN, respectively (Table 1). On the other hand, the bands at 1692 (+)/1673 (−) and 1660 (+)/1646 (−) cm^{-1}, which shift to 1647 (+)/1639 (−) and 1618 (+)/1605 (−) cm^{-1}, respectively, come from amide-I vibrations. From the frequencies, the bands at 1673 and 1646 cm^{-1} in the unphotolyzed state correspond to the loop structure and α-helix, respectively. We previously inferred the protein structural change in the loop and α-helix regions at 150 K (*20*), which is now experimentally unambiguous.

In Figure 6b, the bands at 1730 (+), 1711 (−), and 1687 (+) cm^{-1} were not shifted for ^{13}C-labeling of the protein, which originate from C═O stretching vibrations of FMN. It should be noted that the bands at 1644 (−) and 1629 (+) cm^{-1} apparently look unshifted, suggesting that they are also attributable to the vibrations of FMN such as ring I vibration (*15*, *29*). However, if this is the case, the bands must appear in the spectrum at 150 K because the structural changes of the FMN are similar between 150 and 295 K (Figure 3). No corresponding bands at 150 K (Figure 6a) imply that the bands at 1644 (−) and 1629 (+) cm^{-1} originate from the protein, not from vibrations of FMN.

The bands at 1655 (+), 1644 (−), and 1629 (+) cm^{-1} exhibited isotope effects, presumably shifting to 1614 (+), 1603 (−), and 1588 (+) cm^{-1}, respectively. Similar to that at 150 K, the band at 1678 (−) cm^{-1} was probably split into two bands for ^{13}C-labeling of protein: the remaining band at 1673 (−) cm^{-1} and the shifted band at 1642 (−) cm^{-1}. Interestingly, the blue spectrum shows an additional positive band at 1630 cm^{-1}. The band appears to originate from protein, because the bands at 1644 (−)/1629 (+) cm^{-1} are insensitive to ^{13}C-labeling of FMN (Figure 4b and d). Thus, it is likely that the band at 1655 (+) cm^{-1} was probably split into two bands by the isotope shift, 1630 and 1614 cm^{-1} (Figure 6b). The origins of the bands at 1730 (+)/1711 (−)

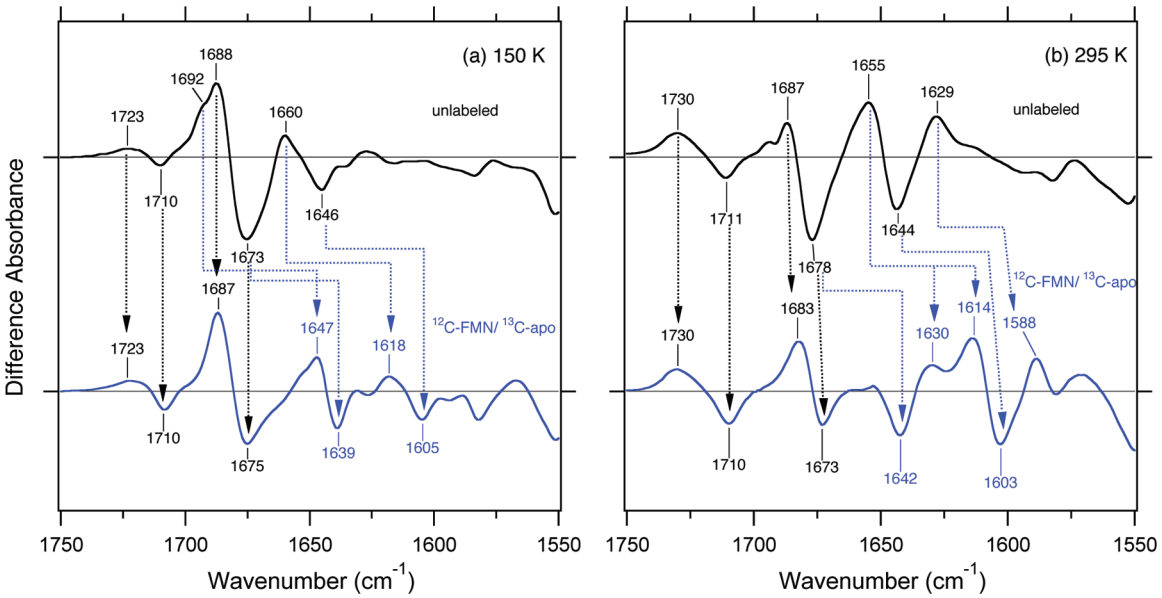

FIGURE 6: Difference FTIR spectra of unlabeled phy3-LOV2 (upper traces) and ^{12}C-FMN/^{13}C-apoprotein phy3-LOV2 (lower traces) in the 1750−1550 cm^{-1} region at 150 K (a) and 295 K (b). The corresponding signals are connected by dotted arrows. One division of the *y*-axis corresponds to 0.014 absorbance units.

and 1687 (+)/1678 (−) cm^{-1} are the C(4)═O and C(2)═O stretching vibrations of FMN, respectively. On the other hand, the bands at 1678 (−)/1655 (+) and 1644 (−)/1629 (+) cm^{-1} originate from amide-I vibrations.

As at 150 K, the successful separation of the bands into those of FMN and protein by using ^{13}C-labeling of protein is advantageous in analyzing protein structural changes at 295 K. There are five peaks for the ^{13}C═O stretching vibrations at 1642 (−), 1630 (+), 1614 (+), 1603 (−), and 1588 (+) cm^{-1} (blue line in Figure 6b). Negative bands at 1642 and 1603 cm^{-1} also appeared at 150 K. Thus, amide-I bands can be assigned as follows. The bands at 1642 (−)/1630 (+) cm^{-1} originate from the amide-I vibration of the loop region, whereas those at 1614 (+)/1603 (−) cm^{-1} come from the amide-I vibration of the α-helix. The additional positive peak at 1588 cm^{-1} at 295 K, not at 150 K, can be assigned to the amide-I vibration of the *β*-sheet. The corresponding negative band is probably located at 1603 (−) cm^{-1}.

DISCUSSION

Reconstitution of phy3-LOV2. We succeeded in the reconstitution of the chromophore and apoprotein of phy3-LOV2 by using the Calumodulin affinity column. Because it was reported that hydrophobic interaction chromatography was used for the reconstitution of oat phot1-LOV2 (*10*, *33*), we tried the same methods. However, phy3-LOV2 remained bound to the pheny-sepharose resin and was not eluted by a low-salt buffer. Many methods have been developed for the reconstitution of flavoproteins (*34*). It was reported that a His-tagged flavoprotein and a Ni-NTA column were used for the reconstitution of flavin (*35*), and we succeeded in the preparation of the CBP-tagged phy3-LOV2 and Calmodulin column at high efficiency. This allowed the FTIR measurements for the reconstituted FMN with reasonable signal-to-noise ratio (Figure 2).

Structural Changes of FMN upon the Activation of phy3-LOV2. During the photocycle of LOV domains, S390 is the only ground-state intermediate (*9*, *12*, *13*). Therefore, it is believed that S390 is the active state for the light-sensing function of phototropin. However, our FTIR study showed a highly temperature-dependent nature for amide-I vibrations of phy3-LOV2 (*20*), suggesting that progressive protein structural changes take place in the S390 state. This conclusion was deduced from the spectral analysis of amide-I vibrations at 1700−1600 cm^{-1}. It should be noted that the frequency region of amide-I vibrations also contains C═O stretching vibrations of FMN, which makes the assignment complicated. In this study, we attempted to separate the C═O stretching vibrations of FMN and protein by using ^{13}C-labeling. ^{13}C-labeling of FMN (4, 10a- and 2-position) or protein allowed us to separate the C═O stretching vibrations of the FMN and peptide backbone (amide-I bands) from each other.

We found that both C(4)═O and C(2)═O stretching vibrations shift to higher frequencies upon the formation of S390, which was essentially temperature-independent. This shows that the hydrogen bonds of the C═O groups are weakened by adduct formation, which presumably relocates the FMN chromophore apart from their hydrogen-bonding donors. The conformational switch of Gln1029 may also contribute to the frequency change in S390. It should be noted, however, that there is a certain temperature-dependence for the C(4)═O and C(2)═O stretching vibrations in the S390 state but in the unphotolyzed state. The frequencies of the C(4)═O stretch in S390 are 1723 and 1730 cm^{-1} at 150 and 295 K, respectively, whereas those of the C(2)═O stretch in S390 are 1687 and 1683 cm^{-1} at 150 and 295 K, respectively (Figure 6). These frequency shifts possibly originate from temperature-dependent chromophore−protein interaction changes.

Structural Changes of Protein upon the Activation of phy3-LOV2. In contrast to the C═O stretching vibrations of FMN, those of the protein (amide-I vibration) are highly temperature-dependent. The hydrogen bond of the peptide backbone in the loop region (1673 cm^{-1}) is weakened at low temper-

atures (1692 cm^{-1}) but is strengthened at room temperature (1655 cm^{-1}). We previously inferred that structural changes in the loop region are relaxed at room temperature from the spectral feature of the amide-I vibration (*20*). Nevertheless, the present study clearly demonstrated that the structure of the loop region changes at 295 K. This change is different from that observed at 150 K. Helical structural perturbation was rather temperature independent, exhibiting a weakened hydrogen bond upon S390 formation (1644 to 1655 cm^{-1}). Cys966 is located at the joint between helical and connected turn structures (Figure 1a). The difference IR spectra at 150 K probably include the structural changes in this region. Interestingly, the blue spectrum in Figure 6a shows that all bands in the 1750−1600 cm^{-1} region shift to higher frequencies upon the formation of S390, such as 1710 to 1723 cm^{-1}, 1675 to 1687 cm^{-1}, 1639 to 1647 cm^{-1}, and 1605 to 1618 cm^{-1}. This indicates weakened hydrogen bonds of the C(4)═O and C(2)═O groups of the FMN and the C═O groups of the peptide backbone. It seems that the formation of a new covalent bond between the chromophore and protein in S390 weakens other chromophore−protein interactions and protein structure, which was observed at 150 K.

At higher temperatures such as 295 K, the secondary structure of the protein is altered from that at 150 K. The hydrogen bond of the loop structure is now strengthened at room temperature, whereas structural changes of the α-helix are similar between those at 150 and 295 K. In addition, the structural perturbation of the *β*-sheet is newly observed only at room temperature. These changes probably correspond to the local-to-global protein structural alterations, and the structure of S390 at 295 K represents the signaling state. It should be noted that the loop structures changing at 150 and 295 K are not necessarily identical in position. We previously identified O−H stretches of the internal water molecules of phy3-LOV2, and the water bands were temperature independent (*36*). These water molecules are bound near Cys966 in the loop region. This may suggest that the loop structure observed at 295 K originates from a different part observed at 150 K.

As is already reported (*20*), the structural perturbation of the *β*-sheet only at 295 K and not at 150 K is an important observation in terms of the signal transduction mechanism. Harper et al. revealed the important role of an extra α-helix at the *C*-terminus for the conformational switch of LOV domains by means of NMR spectroscopy (*22*, *23*). Antiparallel *β*-sheet structure is a common structural motif of the PAS domain (Figure 1a), and the *β*-sheet is sandwiched between the FMN and the *C*-terminal α-helix. An important amino acid, Gln1029, is also located in the *β*-sheet (*5*, *11*). Therefore, the light signal must be transferred from the chromophore domain to the *C*-terminal α-helix by perturbing the *β*-sheet structure. In fact, the mutation of Gln1029 diminishes the secondary structural alteration of the *β*-sheet (*21*), implying the important role of the signal relay pathway.

REFERENCES

1. Liscum, E., and Briggs, W. R. (1995) Mutations in the *NPH1* locus of *Arabidopsis* disrupt the perception of phototropic stimuli, *Plant Cell 7*, 473−485.
2. Kagawa, T., Sakai, T., Suetsugu, N., Oikawa, K., Ishiguro, S., Kato, T., Tabata, S., Okada, K., and Wada, M. (2001) Arabidopsis NPL1: A phototropin homolog controlling the chloroplast high-light avoidance response, *Science 291*, 2138−2141.
3. Kinoshita, T., Doi, M., Suetsugu, N., Kagawa, T., Wada, M., and Shimazaki, K. (2001) phot1 and phot2 mediate blue light regulation of stomatal opening, *Nature 414*, 656−660.
4. Huala, E., Oeller, P. W., Liscum, E., Han, I. -S., Larsen, E., and Briggs, W. R. (1997) Arabidopsis NPH1: A protein kinase with a putative redox-sensing domain, *Science 278*, 2120−2123.
5. Crosson, S., and Moffat, K. (2001) Structure of a flavin-binding plant photoreceptor domain: Insights into light-mediated signal transduction, *Proc. Natl. Acad. Sci. U.S.A. 98*, 2995−3000.
6. Fedorov, R., Schlichting, I., Hartmann, E., Domratcheva, T., Fuhrmann, M., and Hegemann, P. (2003) Crystal structures and molecular mechanism of a light-induced signaling switch: The Phot-LOV1 domain from *Chlamydomonas reinhardtii*, *Biophys. J. 84*, 2474−2482.
7. Salomon, M., Christie, J. M., Knieb, E., Lempert, U., and Briggs, W. R. (2000) Photochemical and mutational analysis of the FMN-binding domains of the plant blue light receptor, phototropin, *Biochemistry 39*, 9401−9410.
8. Miller, S. M., Massey, V., Ballou, D., Williams, C. H., Jr., Distefano, M. D., Moore, M. J., and Walsh, C. T. (1990) Use of a site-directed triple mutant to trap intermediates: Demonstration that the flavin C(4a)-thiol adduct and reduced flavin are kinetically competent intermediates in mercuric ion reductase, *Biochemistry 29*, 2831−2841.
9. Swartz, T. E., Corchnoy, S. B., Christie, J. M., Lewis, J. W., Szundi, I., Briggs, W. R., and Bogomolni, R. A. (2001) The photocycle of a flavin-binding domain of the blue light photoreceptor phototropin, *J. Biol. Chem. 276*, 36493−36500.
10. Salomon, M., Eisenreich, W., Dürr, H., Schleicher, E., Knieb, E., Massey, V., Rüdiger, W., Müller, F., Bacher, A., and Richter, G. (2001) An optomechanical transducer in the blue light receptor phototropin from *Avena sativa*, *Proc. Natl. Acad. Sci. U.S.A. 98*, 12357−12361.
11. Crosson, S., and Moffat, K. (2002) Photoexcited structure of a plant photoreceptor domain reveals a light-driven molecular switch, *Plant Cell 14*, 1067−1075.
12. Kennis, J. T. M., Crosson, S., Gauden, M., van Stokkum, I. H. M., Moffat, K., and van Grondelle, R. (2003) Primary reactions of the LOV2 domain of phototropin, a plant blue-light photoreceptor, *Biochemistry 42*, 3385−3392.
13. Kottke, T., Heberle, J., Hehn, D., Dick, B., and Hegemann, P. (2003) Phot-LOV1: Photocycle of a blue-light receptor domain from the green alga *Chlamydomonas reinhardtii*, *Biophys. J. 84*, 1192−1201.
14. Iwata, T., Tokutomi, S., and Kandori, H. (2002) Photoreaction of the cysteine S-H group in the LOV2 domain of *Adiantum* phytochrome3, *J. Am. Chem. Soc. 124*, 11840−11841.
15. Ataka, K., Hegemann, P., and Heberle, J. (2003) Vibrational spectroscopy of an algal Phot-LOV1 domain probes the molecular changes associated with blue-light reception, *Biophys. J. 84*, 466−474.
16. Bednartz, T., Losi, A., Gärtner, W., Hegemann, P., and Heberle, J. (2004) Functional vibrations among LOV domains as revealed by FT-IR difference spectroscopy, *Photochem. Photobiol. Sci. 3*, 575−579.
17. Iwata, T., Nozaki, D., Tokutomi, S., and Kandori, H. (2005) Comparative investigation of the LOV1 and LOV2 domains in *Adiantum* phytochrome3, *Biochemistry 44*, 7427−7434.
18. Sato, Y., Iwata, T., Tokutomi, S., and Kandori, H. (2005) Reactive cysteine is protonated in the triplet excited state of the LOV2 domain in *Adiantum* phytochrome3, *J. Am. Chem. Soc. 127*, 1088−1089.
19. Nozaki, D., Iwata, T., Tokutomi, S., and Kandori, H. (2005) Unique temperature dependence in the adduct formation between FMN and cysteine S-H group in the LOV2 domain of *Adiantum* phytochrome3, *Chem. Phys. Lett. 410*, 59−63.
20. Iwata, T., Nozaki, D., Tokutomi, S., Kagawa, T., Wada, M., and Kandori, H. (2003) Light-induced structural changes in the LOV2 domain of *Adiantum* phytochrome3 studied by low-temperature FTIR and UV-visible spectroscopy, *Biochemistry 42*, 8183−8191.
21. Nozaki, D., Iwata, T., Ishikawa, T., Todo, T., Tokutomi, S., and Kandori, H. (2004) Role of Gln1029 in the photoactivation processes of the LOV2 domain in *Adiantum* phytochrome3, *Biochemistry 43*, 8373−8379.
22. Harper, S. M., Neil, L. C., and Gardner, K. H. (2003) Structural basis of a phototropin light switch, *Science 301*, 1541−1544.

23. Harper, S. M., Christie, J. M., and Gardner, K. H. (2004) Disruption of the LOV-Jα helix interaction activates phototropin kinase activity, *Biochemistry 43*, 16184−16192.
24. Bowman, W. D., and Spiro, T. G. (1981) Normal mode analysis of lumiflavin and interpretation of resonance Raman spectra of flavoproteins, *Biochemistry 20*, 3313−3318.
25. Schmidt, J., Coudron, P., Thompson, A. W., Watters, K. L., and McFarland, J. T. (1983) Assignment and the effect of hydrogen bonding on the vibrational normal modes of flavins and flavoproteins, *Biochemistry 22*, 76−84.
26. Abe, M., and Kyogoku, Y. (1987) Vibrational analysis of flavin derivatives: Normal coordinate treatments of lumiflavin, *Spectrochim. Acta, Part A 43*, 1027−1038.
27. Livery, C. R., and McFarland, J. T. (1990) Assignment and the effect of hydrogen bonding on the vibrational normal modes pf flavins and flavoproteins, *J. Phys. Chem. 94*, 3980−3994.
28. Zhang, W., Vivoni, A., Lombard, J. R., and Birke, R. L. (1995) Time-resolved SERS study of direct photochemical charge transfer between FMN and a Ag electrode, *J. Phys. Chem. 99*, 12846−12857.
29. Swartz, T. E., Wenzel, P., Corchnoy, S. B., Briggs, W. R., and Bogomolni, R. A. (2002) Vibration spectroscopy reveals light-induced chromophore and protein structural changes in the LOV2 domain of the plant blue-light receptor phototropin 1, *Biochemistry 41*, 7183−7189.
30. Miura, R., Nishina, Y., Ohta, M., Tojo, H., Shiga, K., Watari, H., Yamano, T., and Miyake, Y. (1983) Resonance Raman study on the flavin in the purple intermediates of D-amino acid oxydase, *Biochem. Biophys. Res. Commun. 111*, 588−594.
31. Hazekawa, I., Nishina, Y., Sato, K., Shichiri, M., Miura, R., and Shiga, K. (1997) A Raman study on the C(4)═O stretching mode of flavins in flavoenzymes: Hydrogen bonding at the C(4)═O moiety, *J. Biochem. 121*, 1147−1154.
32. Kitagawa, T., Nishina, Y., Kyogoku, Y., Yamano. T., Onishi, N., Takai-Suzuki, A., and Yagi, K. (1979) Resonance Raman spectra of carbon-13- and nitrogen-15-labeled riboflavin bound to egg-white flavoprotein, *Biochemistry 18*, 1804−1808.
33. Dürr, H., Salomon, M., and Rüdiger, W. (2005) Chromophore exchange in the LOV2 domain of the plant photoreceptor phototropin from oat, *Biochemistry 44*, 3050−3055.
34. Hefti, M. H., Vervoort, J., and van Berkel, W. J. H. (2003) Deflavination and reconstitution of flavoproteins tackling fold and function, *Eur. J. Biochem. 270*, 4227−4242.
35. Hefti, M. H., Milder, F. J., Boeren, S., Vervoort, J., and van Berkel, W. J. H. (2003) A His-tag based immobilization method for the preparation and reconstitution of apoflavoproteins, *Biochim. Biophys. Acta 1619*, 139−143.
36. Nozaki, D., Iwata, T., Tokutomi, S., and Kandori, H. (2005) Water structural changes in the activation process of the LOV2 domain of Adiantum phytochrome3, *J. Mol. Struct. 735/736*, 259−265.

BI061837V